

Kinematics estimation of straddled movements on high bar from a limited number of skin markers using a chain model

Mickael Begon, Pierre-Brice Wieber, Maurice Raymond Yeadon

► **To cite this version:**

Mickael Begon, Pierre-Brice Wieber, Maurice Raymond Yeadon. Kinematics estimation of straddled movements on high bar from a limited number of skin markers using a chain model. *Journal of Biomechanics*, Elsevier, 2008, 41 (3), pp.581-586. <10.1016/j.jbiomech.2007.10.005>. <inria-00390475>

HAL Id: inria-00390475

<https://hal.inria.fr/inria-00390475>

Submitted on 2 Jun 2009

HAL is a multi-disciplinary open access archive for the deposit and dissemination of scientific research documents, whether they are published or not. The documents may come from teaching and research institutions in France or abroad, or from public or private research centers.

L'archive ouverte pluridisciplinaire **HAL**, est destinée au dépôt et à la diffusion de documents scientifiques de niveau recherche, publiés ou non, émanant des établissements d'enseignement et de recherche français ou étrangers, des laboratoires publics ou privés.

Kinematics estimation of straddled movements on high bar from a limited number of skin markers using a chain model

Mickaël Begon ^{a,*}, Pierre-Brice Wieber ^b,

Maurice Raymond Yeadon ^a

^aSchool of Sport and Exercise Sciences, Loughborough University

Loughborough Leics. LE11 3TU

United Kingdom

^bINRIA Rhône-Alpes, Inovallée 655 avenue de l'Europe, Montbonnot 38 334 Saint

Ismier Cedex France

Revision 1 with minor corrections.

Address for correspondence: Dr M. Begon

School of Sport and Exercise Sciences

Loughborough University

Ashby Road – Loughborough

Leicestershire LE11 3TU

United Kingdom

1 **Abstract**

2 To reduce the effects of skin movement artefacts and apparent joint dislocations
3 in the kinematics of whole body movement derived from marker locations, global
4 optimisation procedures with a chain model have been developed. These procedures
5 can also be used to reduce the number of markers when self-occlusions are hard
6 to avoid. This paper assesses the kinematics precision of three marker sets: 16,
7 11 and 7 markers, for movements on high bar with straddled piked posture. A
8 three-dimensional person-specific chain model was defined with 9 parameters and
9 12 degrees of freedom and an iterative procedure optimised the gymnast posture for
10 each frame of the three marker sets. The time histories of joint angles obtained from
11 the reduced marker sets were compared with those from the 16 marker set by means
12 of a root mean square difference measure. Occlusions of medial markers fixed on the
13 lower limb occurred when the legs were together and the pelvis markers disappeared
14 primarily during the piked posture. Despite these occlusions, reconstruction was
15 possible with 16, 11 and 7 markers. The time histories of joint angles were similar;
16 the main differences were for the thigh mediolateral rotation and the knee flexion
17 because the knee was close to full extension. When five markers were removed, the
18 average angles difference was about 3° . This difference increased to 9° for the seven
19 marker set. It is concluded that kinematics of sports movement can be reconstructed
20 using a chain model and a global optimisation procedure for a reduced number of
21 markers.

22 *Key words:* kinematics, chain model, gymnastics, optimisation

* Corresponding author.

Email address: M.Begon@lboro.ac.uk (Mickaël Begon).

23 Kinematics estimation of straddled movements on high
24 bar from a limited number of skin markers using a chain
25 model

26 **1 Introduction**

27 In sports biomechanics, as in clinical gait analysis, optoelectronic motion cap-
28 ture systems based on passive markers are widely used to recover human move-
29 ment descriptors. The poses (position and orientation) of the body segments
30 are determined from skin-mounted markers before their kinematics and kinet-
31 ics are calculated. In the direct approach (Kadaba et al., 1990), at least three
32 markers per segment are needed for the definition of a segment-embedded ref-
33 erence frame which represents the pose of the segment. This approach has
34 numerous limitations associated with the number of markers and the use of a
35 rigid segment representation. Moreover the kinematics remains inaccurate be-
36 cause no compensation is made for the skin movement artefacts (Reinschmidt
37 et al., 1997a).

38 The kinematics accuracy can be improved by increasing the number of markers
39 per segment (Challis, 1995). The calculation of the rotation matrices from five
40 markers seems to be a good compromise to limit the damaging effect of skin
41 movement artefacts. In clinical analysis, there exist marker sets (Davis et al.,
42 1991) which are used to minimize the number of markers. Joint centres are
43 defined from static data acquisitions or from measurements on the participant.
44 These marker sets are based on assumptions which allow the medial markers
45 to be removed during walking trials. For these marker sets, the joint centre
46 location is estimated with a predictive approach based on anthropometrical

47 measurement or the midpoint of two markers.

48 Human kinetics calculation is often based on multibody dynamics assuming
49 pin joints without translation. However with at least three markers, each body
50 segment can be considered independently of the proximal one and will have
51 three degrees of freedom (DoF) in rotation and three DoF in translation.
52 Kinematic and kinetic parameters are calculated from non-rigid arrays of
53 markers and procedures have been developed to limit the array deformation
54 (Chèze et al., 1995; Spoor and Veldpaus, 1980). In these formulations, each
55 segment is treated independently without guaranteeing a constant segment
56 length. To reduce skin movement artefacts and apparent joint dislocations, Lu
57 and O'Connor (1999) proposed a global optimisation procedure with a chain
58 model. This method has been applied to computer simulated movements of
59 the lower limbs (Lu and O'Connor, 1999) and the upper limbs (Roux et al.,
60 2002). Other chain models associated with optimisation procedures have been
61 used to analyse gait (Charlton et al., 2004; Reinbolt et al., 2005). In Reinbolt
62 et al. (2005) the determination of the kinematics was based on a two-level
63 optimisation and required three markers per segment. Performance measures
64 of this algorithm were estimated for 12- DoF synthetic motions.

65 In contrast with gait analysis, no standard marker set can be used satisfactorily
66 for data collection in sport. Each movement has its own segment deformations
67 arising from muscle contractions and joint motions together with its own self-
68 occlusions that require a specific marker set. Additionally, the use of three or
69 more markers per segment is impractical for whole body sports movements
70 because of increased marker occlusion, increased soft tissue movement and
71 increased marker detachment during dynamic movements.

72 Usually the joints are modelled as ball-and-socket (*e.g.* hip joint or gleno-
73 humeral joint) or as hinge joints (*e.g.* knee). If the joint centre location is
74 known then there is some redundancy in using three markers since two will
75 suffice for a three *DoF* joint and one marker will suffice for a single *DoF* joint.
76 The purpose of this study was to determine the kinematics of a movement
77 from a limited number of markers and the definition of a person-specific chain
78 model.

79 2 Methods

80 A 9-parameter, 3-dimensional, 12-*DoF* model was used to describe the kine-
81 matics of circling movements with a piked and straddled posture on the high
82 bar in gymnastics. This chain model was designed for this specific applica-
83 tion, but the method allows any model to be defined. Twenty-two technical
84 and anatomical reflective markers were used to define the chain model. Kine-
85 matics was calculated from 16, 11 and 7 markers and then the three sets were
86 compared to quantify the effect of the marker number. The model implemen-
87 tation and the kinematics optimisation from real data were performed using
88 the *HuMANs* toolbox under Scilab (Wieber et al., 2006).

89 The body was considered as an articulated system composed of rigid bodies
90 corresponding to the following segments: upper limbs, scapular girdle, torso-
91 head, pelvis, right thigh, left thigh, right shank-foot and left shank-foot. The
92 kinematics of the left and right lower-limbs was viewed as being symmetri-
93 cal. Six parameters (p_i) and 12 *DoF* (q_i) described the chain model (Fig. 1).
94 Flexion, abduction and lateral rotation were defined to be positive and the
95 angle sequence was flexion-extension, abduction-adduction and mediolateral

96 rotation.

97 [Fig. 1 about here.]

98 The participant, a member of the Great Britain Men’s Senior Gymnastics
99 Squad (17 years, 61.6 kg, 1.705 m), gave informed consent to perform a number
100 of straddled stalders and endos on the high bar (Fig. 2) changing technique
101 and velocity from trial to trial. Ten successful trials of each of the two circling
102 movements were selected for analysis.

103 [Fig. 2 about here.]

104 All trials were captured using 18 Vicon cameras operating at 100 Hz and
105 positioned on a hemisphere on the left side of the subject. A volume centred
106 on the high bar spanning $3\text{ m} \times 5\text{ m} \times 5\text{ m}$ was wand calibrated. Twenty-
107 one spherical markers of 25 mm diameter were attached to the trunk and
108 the left upper and lower limbs: lateral and medial malleolus ($T_{1,2}$), tibia (T_3),
109 lateral and medial knee ($T_{4,5}$), lateral side of the mid-thigh (T_6), left and
110 right anterior superior iliac spines ($T_{7,8}$), left and right posterior superior iliac
111 spines ($T_{9,10}$), xyphoid (T_{11}), manubrium (T_{12}), first thoracic vertebra (T_{13}),
112 a rigid tripod fixed on the acromion (T_{14-16}), under the deltoid (T_{17}), medial
113 side of the elbow (T_{18}), olecran (T_{19}), and lateral and medial wrist ($T_{20,21}$).
114 One additional marker was placed at the middle of the bar (T_{22}) between the
115 hands. Markers T_{14-16} were removed before the data collection for the circling
116 movements.

117 The dimensions of the model and the marker locations with respect to (*wrt*)
118 the local segment reference frame had to be determined accurately. These
119 required the determination of the centre of rotation (CoR) location and the

120 definition of the local frame associated with each body segment. Predictive
121 and functional approaches were used involving static and dynamic data ac-
122 quisition. The glenohumeral and hip CoR (modelled as ball and socket) were
123 located with the symmetrical CoR estimation method (Ehrig et al., 2006)
124 in line with the recommendation of Begon et al. (2007) and Monnet et al.
125 (in press) from markers T_{14-19} and T_{3-10} respectively. The pelvis local frame
126 was calculated from four markers (T_{7-10}) using an optimisation procedure
127 (Challis, 1995). The elbow, wrist, knee, and ankle CoR (modelled as hinge
128 joints) were determined as the midpoint of lateral and medial markers. The
129 torso CoR relative to the pelvis was defined according to the anthropometri-
130 cal model of Yeadon (1990). Then the parameters were personalised for the
131 gymnast from the CoR locations during a static trial in anatomical posture.
132 Arm flexion causes elevation of the glenohumeral joint due to rotation about
133 the sternoclavicular joint. An initial position of the glenohumeral joint *wrt*
134 the torso frame was determined using the static trial data. From a trial with
135 arm flexion-extension motion, the scapular girdle elevation was modelled as
136 a linear function f of the arm flexion q_7 . The location of each marker was
137 expressed in the local frame of the corresponding body segment and these
138 locations were introduced into the model.

139 From the data acquisition of stalders and endos on high bar, the generalized
140 coordinates (q_{1-12}) were optimised for each frame. The resulting global op-
141 timisation was a non-linear programming problem so it had to be evaluated
142 numerically using iterative optimisation methods (a Newton-Gauss non-linear
143 least square algorithm). The reconstruction process was static; each posture
144 was determined independently from the one before. Ideally we would like to
145 obtain the generalized position vector $\mathbf{q} = q_{1-12}$ such that: $T_{ags}(\mathbf{q}) = \mathbf{T}$,

146 where $Tags(\mathbf{q})$ is the forward kinematics function of the chain model and
 147 $\mathbf{T} = T_{1-13,17-22}$ is the matrix of the observed marker positions. Based on the
 148 Jacobian of the $Tags$ ($\partial T_i/\partial q_j$), the generalized co-ordinates were iteratively
 149 optimised in order to minimize $\|Tags(\mathbf{q}) - \mathbf{T}\|^2$.

150 Three sets of kinematics were calculated using the chain model with, for
 151 each segment, three markers (Kin_{16}): $T_{1-7,9-13,19-22}$, two markers (Kin_{11}):
 152 $T_{1,3,4,6,7,9,11,13,19,21,22}$ or only one marker except for the pelvis with two markers
 153 (Kin_7): $T_{1,4,7,9,11,19,22}$. Kin_{16} was considered as the reference marker set. As
 154 skin deformation occurs in areas closer to the joints (Cappozzo et al., 1996),
 155 the markers used for Kin_{11} and Kin_7 were chosen far from joints with large
 156 ranges of motion (shoulder, hip, back).

For each set of kinematics, the global error of reconstruction was defined by:

$$\frac{1}{M} \sum_{M=1}^M \frac{1}{F_m} \sum_{f=1}^{F_m} \sqrt{\frac{1}{3 \times N_{f,m}} \sum_{n=1}^{N_{f,m}} -12\|Tags(\mathbf{q}) - \mathbf{T}\|^2},$$

157 where M is the number of trials, F_m is the number of frames for trial m
 158 and $N_{f,m}$ is the numbers of visible markers for frame f in trial m . The time
 159 histories of each generalized co-ordinate were compared by means of a root
 160 mean square difference (RMSD). RMSD of Kin_7 and Kin_{11} relative to Kin_{16}
 161 were compared by means of a paired t -test ($p < 0.05$).

162 **3 Results**

163 The reconstructions were processed in 57 ± 14 ms, 44 ± 9 ms and 131 ± 31 ms for
 164 one frame of data and the global errors of reconstruction were 26.7 ± 3.0 mm,
 165 26.7 ± 3.4 mm and 31.4 ± 2.5 mm for Kin_{16} , Kin_{11} and Kin_7 respectively.

166 Whatever the trial, this error estimate decreased from Kin_{16} to Kin_{11} as
167 well as from Kin_{11} to Kin_7 . The marker occlusions varied from 0% to 65%
168 of the total number of frames depending on the marker (Table 1). There
169 were no occlusions for the markers $T_{1,3,4,6,9,11,18,19,21,22}$. The occlusion number
170 of the other markers could reach half the frames (T_8) or exceed it ($T_{5,10}$).
171 The occlusions of the markers fixed on the medial side of the lower left limb
172 occurred when the legs were together, and the pelvis markers disappeared
173 mainly during the piked posture. For Kin_7 the markers were reconstructed in
174 all the frames for the 20 movements except for the left anterior superior iliac
175 spine T_7 which had 22% occlusions ($\pm 6\%$). Among the markers used for Kin_{11} ,
176 the first thoracic vertebra marker T_{13} also had a few occlusions ($4 \pm 7\%$).

177 [Table 1 about here.]

178 In general, the joint angles calculated from the three marker sets were similar
179 (Fig. 3). The main differences were for the thigh mediolateral rotation (q_{11})
180 and the knee flexion (q_{12}). The RMSD of the joint angles over the 20 circling
181 movements ranged from 1° to 39° (Table 2). The RMSD of the arm rotation
182 about the bar q_4 for Kin_{11} and Kin_7 relative to Kin_{16} never exceeded 2.2° .
183 For Kin_{11} the maximum RMSD of the angles was less than 13.0° and the
184 average RMSD was about 3.7° . The maximum values were found for the thigh
185 mediolateral rotation (q_{11}). For Kin_7 this angle was imprecise with an average
186 RMSD of 39° for a 56° range of motion. The other angles had an average
187 difference of 4° . The RMSD of the prismatic joints ($q_{5,6}$) remained less than
188 6 mm for Kin_{11} and were in the order of a centimetre for Kin_7 .

189 [Fig. 3 about here.]

190 [Table 2 about here.]

191 Only the RMSD of q_5 (translation of the arm *wrt* the bar) did not change
192 significantly ($p = 0.49$) with the number of markers (Table 2). The other
193 co-ordinates differed significantly ($p < 0.001$); the RMSD values increased
194 systematically with a reduction in marker number. On average, the RMSD
195 values for Kin_7 and Kin_{11} differed by less than 4° for $q_{4,7,8,9,10,12}$ and by 9 mm
196 for q_6 . The main change was the thigh mediolateral rotation where the RMSD
197 increased from 10° to 39° when $T_{3,6}$ were removed in the change from Kin_{11}
198 to Kin_7 .

199 4 Discussion

200 The purpose of this study was (*i*) to apply a global optimisation on a fast
201 movement with large range of motion and (*ii*) to reduce the number of mark-
202 ers for the kinematics reconstruction. A 9-parameter, 3-dimensional, 12-*DoF*
203 chain model was shown to be suitable for modelling straddled movements on
204 high bar and the kinematics reconstruction was precise with 11 markers or 7
205 markers except for the thigh mediolateral rotation.

206 The proposed model seems to be a reasonable compromise between accuracy
207 and simplicity of gymnast description for movements on high bar. The model
208 was defined after observation, analyses and knowledge about circling move-
209 ments on high bar (Hiley and Yeadon, 2003, 2005). On one hand, the kine-
210 matics is constrained by the gymnastics rules (*i.e.* symmetrical movements,
211 full extension of some joints); on the other hand the kinematics of the shoul-
212 der is complex and the body length increases due to the high internal forces
213 associated with the centripetal accelerations.

214 For simplicity of the model, the foot and head segments were considered to
215 be fixed *wrt* the shank and the torso respectively and the elbow was kept
216 fully extended. In gymnastics, the foot has to be aligned with the shank and
217 the lower-arm aligned with the upper-arm. The small amplitude of rotation
218 of these joints could have only a small effect on the dynamics. Simple ball
219 and socket or hinge joints do not model the real musculoskeletal system ac-
220 curately (Lu and O'Connor, 1999); joint models that are more anatomical
221 can be defined. The previous gymnast models for high bar movements (Hiley
222 and Yeadon, 2003, 2005) have been improved by introducing an extra *DoF* be-
223 tween the torso and the pelvis and by a personalised behaviour of the scapular
224 girdle elevation as a function of arm flexion (q_7). The elevation of the scapular
225 girdle could not be estimated by the global optimisation procedure because it
226 would cause a singularity with q_6 (arm lengthening) when $q_7 = 0 \pm \pi$ (shoulder
227 flexion), *i.e.* if arm and trunk were aligned. The joint location in the back was
228 determined from observation of the whole spine flexion and according to the
229 anthropometrical model of Yeadon (1990). This chain model defined for me-
230 chanical analysis and optimisation of circling movement with piked straddled
231 postures has to be associated with an anthropometrical model to calculate the
232 kinetics.

233 The main experimental problem of straddled movements on high bar was the
234 marker occlusions. Despite using 18 cameras, there were a lot of occlusions for
235 the markers fixed on the medial side of the limbs ($T_{2,4,18,20}$) or on the right
236 side of the pelvis ($T_{8,10}$). The pelvis markers were also affected by the piked
237 posture. This explained 21% of occlusions for the left anterior superior iliac
238 spine marker T_7 . A general placement of cameras cannot solve the problem
239 of occlusions since a specific placement for each athlete and each movement

240 is needed. Many athletic movement analyses would be impaired if at least
241 three markers were required to define each segment, because marker occlusions
242 could not be avoided and marker interpolation for movements involving high
243 acceleration can result in kinematics with large errors. This approach based
244 on a chain model compensates for marker occlusion.

245 The reference kinematics was chosen as the result of the global optimisation
246 with 16 markers (Kin_{16}) rather than the *direct approach* (Kadaba et al., 1990).
247 In line with the works of Lu and O'Connor (1999) and Roux et al. (2002),
248 global optimisation is more accurate than the *direct approach*. While these
249 studies were based on computer simulated trials, the noise added to the marker
250 kinematics was systematic (Chèze et al., 1995), this being more appropriate to
251 model skin movement artefacts than random noise as confirmed by Begon et al.
252 (2007). Furthermore in the present study, the direct method could be applied
253 for only a few frames due to the marker occlusions throughout the movement
254 (Table 1). The global optimisation works with any prior defined kinematic
255 model structure and any experimental movement data without any restriction
256 on the marker number and location while the Hessian remains of full rank.
257 The *HuMANs* toolbox (Wieber et al., 2006) allows new model chains to be
258 implemented in order to reconstruct accurately the kinematics of movement
259 with marker occlusions. The present algorithm will be improved in the future
260 by introducing a weighting matrix in the Hessian and Jacobian expression and
261 by a Kalman filter.

262 The precision of the kinematics obtained with the present algorithm was cal-
263 culated for three sets of markers. The global error of reconstruction was about
264 27 mm for Kin_{16} and Kin_{11} . The global error increased to 31 mm for Kin_7 .
265 The optimisation procedure always found a solution which depended on data

266 accuracy and redundancy. Using redundant information (Kin_{16} and Kin_{11}),
267 the chain model and markers compensated for each other's error. Since the
268 error did not increase between Kin_{16} and Kin_{11} , the latter set of markers
269 seemed to be a good compromise between the number of markers and their
270 position to avoid skin movement artefacts. Global optimization provides a
271 great opportunity to design optimal marker sets to minimize skin movement
272 artefact, because less than three markers are needed on each body segment
273 and the noisy markers can be removed.

274 The RMSDs found in this study for the thigh angles (q_{9-11}) could be dis-
275 cussed in line with the errors measured using intra-cortical pins (Reinschmidt
276 et al., 1997a,b; Karlsson and Lundberg, 1994). In running (Reinschmidt et al.,
277 1997b) the errors expressed as a percentage of the range of motion were 21%
278 for flexion-extension, 64% for abduction-adduction and 70% for mediolateral
279 rotation of the thigh. These RMSDs during the circling movement with Kin_{11}
280 on high bar corresponded to 2%, 1% and 18% of the thigh ranges of motion.
281 For Kin_7 , the RMSDs increased to 5%, 5% and 71%. Whatever the move-
282 ment, the error associated with the mediolateral rotation of the thigh is the
283 greatest. The study of Karlsson and Lundberg (1994) showed a difference of
284 about 30° for the thigh mediolateral rotation calculated with skin-attached
285 and bone-anchored markers (50° versus 20°). With global optimisation, the
286 less noisy markers of pelvis and shank help to bring the thigh mediolateral
287 rotation toward the correct orientation (Lu and O'Connor, 1999). The chain
288 model and marker redundancy play an important role in compensating for
289 errors. In this study, when the number of markers was reduced, the redun-
290 dancy decreased and the inaccuracy increased. Since the knee was close to
291 full extension, the mediolateral rotation (q_{11}) was poorly compensated for by

292 the markers on the shank. The imprecision of q_{11} will have a small effect on
293 the dynamics of straddled movements on high bar with straight legs. As the
294 changes in knee flexion is small ($\Delta q_{12} \approx 10^\circ$) and as the knee should be fully
295 extended in gymnastics, some assumptions could be introduced into the chain
296 model for a reconstruction with seven markers. The thigh mediolateral rota-
297 tion and knee flexion could be assumed to be zero throughout the movement.
298 An alternative would be to express q_{11} as a function of thigh flexion-extension
299 and abduction-adduction.

300 In conclusion, kinematics can be reconstructed with a chain model and a
301 global optimisation procedure for a reduced number of markers. The chain
302 model makes the most of the information contained in all the markers. In the
303 case of circling movements on high bar with a piked straddled posture, 11
304 markers allowed a 12-*DoF* model to be reconstructed within a 3° , 4 mm error.
305 With the modifications suggested above it should be possible to obtain good
306 results with 7 markers. Future studies will be based on the simplification of
307 the model by expressing the trunk flexion and the thigh mediolateral rotation
308 as functions of thigh flexion-extension and abduction-adduction.

309 5 Conflict of interest statement

310 There are no conflicts of interest to declare by the authors.

311 6 Acknowledgements

312 The authors wish to acknowledge the support of the British Gymnastics
313 World Class Programme and EGIDE (Ministère des Affaires Etrangères, France).

314 References

315 Begon, M., Monnet, T., Lacouture, P., 2007. Effects of movement for estimat-
316 ing the hip joint centre. *Gait & Posture* 25, 353–359.

317 Cappozzo, A., Catani, F., Leardini, A., Benedetti, M., Croce, U. D., 1996.
318 Position and orientation in space of bones during movement: experimental
319 artefacts. *Clinical Biomechanics* 11, 90–100.

320 Challis, J. H., 1995. A procedure for determining rigid body transformation
321 parameters. *Journal of Biomechanics* 28, 733–737.

322 Charlton, I. W., Tate, P., Smyth, P., Roren, L., 2004. Repeatability of an
323 optimised lower body model. *Gait & Posture* 20, 213–221.

324 Chèze, L., Fregly, B. J., Dimnet, J., 1995. A solidification procedure to facili-
325 tate kinematic analyses based on video system data. *Journal of Biomechan-*
326 *ics* 28, 879–884.

327 Davis, R., Ounpuu, S., Tyburski, D., Gage, J., 1991. A gait analysis data
328 collection and reduction technique. *Human Movement Science* 10, 575–587.

329 Ehrig, R. M., Taylor, W. R., Duda, G. N., Heller, M. O., 2006. A survey of
330 formal methods for determining the centre of rotation of ball joints. *Journal*
331 *of Biomechanics* 39, 2798–2809.

332 Hiley, M., Yeadon, M., 2003. Optimum technique for generating angular mo-
333 mentum in accelerated backward giant circles prior to a dismount. *Journal*
334 *of Applied Biomechanics* 19, 119–130.

335 Hiley, M., Yeadon, M., 2005. The margin for error when releasing the asym-
336 metric bars for dismounts. *Journal of Applied Biomechanics* 21, 223–235.

337 Kadaba, M., Ramakrishnan, H., Wootten, M., 1990. Measurement of lower
338 extremity kinematics during level walking. *Journal of Orthopaedic Research*
339 8, 383–392.

340 Karlsson, D., Lundberg, A., 1994. Accuracy estimation of kinematic data de-
341 rived from bone anchored external markers. In *Proceedings of the 3rd In-*
342 *ternational Symposium on 3-D Analysis of Human Motion.*

343 Lu, T.-W., O’Connor, J., 1999. Bone position estimation from skin marker
344 co-ordinates using global optimisation with joint constraints. *Journal of*
345 *Biomechanics* 32, 129–134.

346 Monnet, T., Desailly, E., Begon, M., Vallee, C., Lacouture, P., (in press) Com-
347 parison of the score and ha methods for locating in vivo the glenohumeral
348 joint centre. *Journal of Biomechanics.*

349 Reinbolt, J. A., Schutte, J. F., Fregly, B. J., Koh, B. I., Haftka, R. T., George,
350 A. D., Mitchell, K. H., 2005. Determination of patient-specific multi-joint
351 kinematic models through two-level optimization. *Journal of Biomechanics*
352 38, 621–626.

353 Reinschmidt, C., Bogert, A., Lundberg, A., Nigg, B., Murphy, N., Stacoff, A.,
354 Stano, A., 1997a. Tibiofemoral and tibiocalcaneal motion during walking:
355 external vs. skeletal markers. *Gait & Posture* 6, 98–109.

356 Reinschmidt, C., Bogert, A., Nigg, B., Lundberg, A., Murphy, N., 1997b. Ef-
357 fect of skin movement on the analysis of skeletal knee joint motion during
358 running. *Journal of Biomechanics* 30, 729–732.

359 Roux, E., Bouilland, S., Godillon-Maquinghen, A.-P., Bouttens, D., 2002.
360 Evaluation of the global optimisation method within the upper limb kine-
361 matics analysis. *Journal of Biomechanics* 35, 1279–1283.

- 362 Spoor, C., Veldpaus, F., 1980. Rigid body motion calculated from spatial
363 coordinates markers. *Journal of Biomechanics* 13, 391–393.
- 364 Wieber, P.-B., Billet, F., Boissieux, L., Pissard-Gibollet, R., 2006. The hu-
365 mans toolbox, a homogeneous framework for motion capture, analysis and
366 simulation. In: *Ninth International Symposium on the 3D analysis of human
367 movement*.
- 368 Yeadon, M. R., 1990. The simulation of aerial movement–II. A mathematical
369 inertia model of the human body. *Journal of Biomechanics* 23, 67–74.

371	1	Model definition with the degrees of freedom and the	
372		parameters for the straddled circling movements on high	
373		bar. Degrees of freedom: q_{1-3} translation of the bar, q_4 arm	
374		rotation, q_5 arm translation, q_6 arm lengthening, q_7 shoulder	
375		flexion, q_8 , spinal flexion, q_9 thigh flexion, q_{10} thigh abduction,	
376		q_{11} thigh lateral rotation and q_{12} knee flexion. Parameters:	
377		p_1 arm length, p_2 torso length, p_3 half-width of the pelvis, p_4	
378		pelvis height, p_5 knee adduction and p_6 thigh length.	19
379	2	Straddled stalder (a) and endo (b) on high bar.	20
380	3	Time histories of the generalized co-ordinates for an endo	
381		calculated with 16, 11 and 7 markers.	21

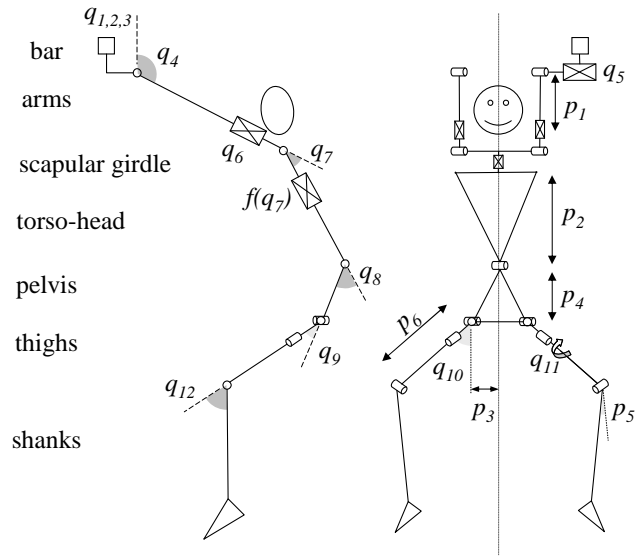


Fig. 1. Model definition with the degrees of freedom and the parameters for the straddled circling movements on high bar. Degrees of freedom: q_{1-3} translation of the bar, q_4 arm rotation, q_5 arm translation, q_6 arm lengthening, q_7 shoulder flexion, q_8 , spinal flexion, q_9 thigh flexion, q_{10} thigh abduction, q_{11} thigh lateral rotation and q_{12} knee flexion. Parameters: p_1 arm length, p_2 torso length, p_3 half-width of the pelvis, p_4 pelvis height, p_5 knee adduction and p_6 thigh length.

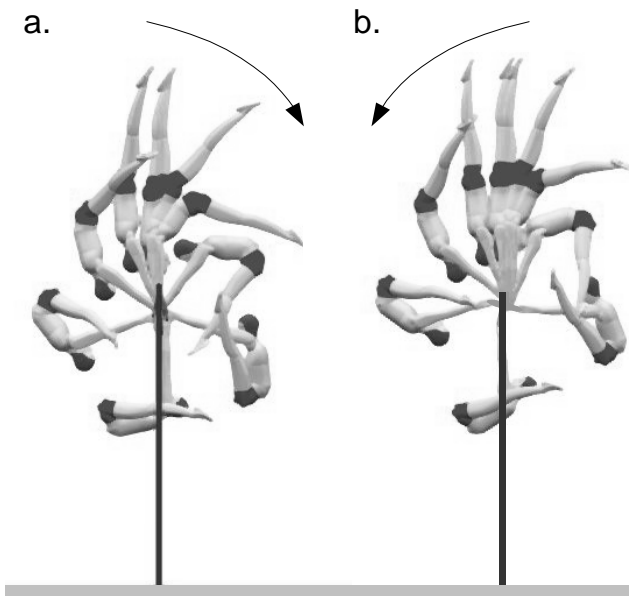


Fig. 2. Straddled stalder (a) and endo (b) on high bar.

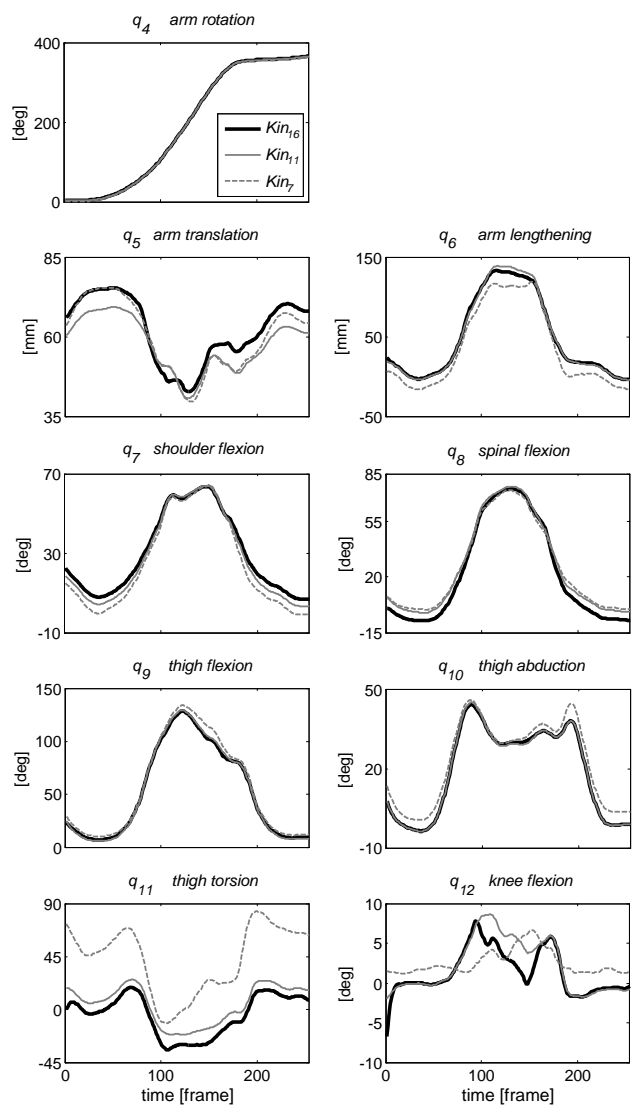


Fig. 3. Time histories of the generalized co-ordinates for an endo calculated with 16, 11 and 7 markers.

383	1	Marker occlusions during the circling movements	23
384	2	Root mean square difference for each global co-ordinate	
385		of Kin_{11} and Kin_7 relative to Kin_{16} , with notation	
386		$Kin_{11/16}$, $Kin_{7/16}$ respectively	24

Table 1
 Marker occlusions during the circling movements

		mean	SD
Shank	T_1	0	(0)
	T_2	9	(17)
	T_3	0	(0)
Thigh	T_4	0	(0)
	T_5	65	(11)
	T_6	0	(0)
Pelvis	T_7	22	(6)
	T_8	42	(8)
	T_9	0	(0)
	T_{10}	56	(14)
Torso	T_{11}	0	(0)
	T_{12}	1	(2)
	T_{13}	4	(7)
Upper-limb	T_{17}	6	(6)
	T_{18}	0	(0)
	T_{19}	0	(0)
	T_{20}	6	(6)
	T_{21}	0	(0)
Bar	T_{22}	0	(0)

Note: the average values and the standard deviations are expressed as a percentage of the number of frames.

Table 2

Root mean square difference for each global co-ordinate of Kin_{11} and Kin_7 relative to Kin_{16} , with notation $Kin_{11/16}$, $Kin_{7/16}$ respectively

	q_i	Unit	$Kin_{11/16}$	$Kin_{7/16}$	p	RoM
Arm Rotation	4	[°]	0.5 ± 0.1	1.3 ± 0.3	< 0.001	457 ± 154
Arm Translation	5	[mm]	4.1 ± 1.2	4.4 ± 1.9	0.49	33 ± 7
Arm Lengthening	6	[mm]	3.3 ± 0.6	12.3 ± 2.6	< 0.001	158 ± 18
Shoulder Flexion	7	[°]	2.1 ± 0.5	4.9 ± 1.0	< 0.001	64 ± 11
Spinal Flexion	8	[°]	3.5 ± 0.9	4.4 ± 1.2	< 0.001	87 ± 12
Thigh Flexion	9	[°]	2.0 ± 0.5	6.0 ± 1.7	< 0.001	131 ± 9
Thigh Abduction	10	[°]	0.6 ± 0.1	2.6 ± 0.8	< 0.001	53 ± 7
Thigh torsion	11	[°]	10.0 ± 1.2	38.9 ± 7	< 0.001	56 ± 5
Knee Flexion	12	[°]	2.6 ± 0.7	4.8 ± 2.1	< 0.001	20 ± 8

Note: the fifth column is the p -value of the paired t -test between $Kin_{11/16}$ and $Kin_{7/16}$. The last column is the range of motion (RoM) calculated with Kin_{16} .